



# On the Future Role of the most Parsimonious Climate Module in Integrated Assessment

Mohammad M. Khabbazan and Hermann Held

5 Research Unit Sustainability and Global Change, Center for Earth System Research and Sustainability, Universität Hamburg, Grindelberg 5, 20144 Hamburg, Germany

*Correspondence to:* Mohammad M. Khabbazan (mohammad.khabbazan@uni-hamburg.de)

**Abstract.** We test the validity of a one-box climate model as an emulator for Atmosphere-Ocean General Circulation Models (AOGCMs) when the application is confined to the subset of scenarios approximately in-line with the 2° target. The one-box climate model is currently in use in the integrated assessment models FUND and MIND. For our assessment, we 10 crucially rely on 14 recent CMIP5 AOGCM diagnostics of the total radiative forcing for various representative concentration pathways. Our findings are two-fold. Firstly, when directly prescribing AOGCMs' respective equilibrium climate sensitivities (ECSs) and transient climate responses (TCRs) to the one-box model, global mean temperature (GMT) projections are generically too large by 0.5 K at peak temperature. Accordingly, corresponding integrated assessment studies might overestimate mitigation need and cost. Secondly, the one-box model becomes an excellent emulator of those 15 AOGCMs once their ECS and TCR values are universally mapped onto effective one-box intrinsic counterparts. We suggest utilizing this one-box model in integrated assessment also in the future, in particular when computationally demanding decision-making under climate response uncertainty continues to be modelled. However, then the roles of ECS and TCR must be re-interpreted. For the MIND model as used over the past 5 years, even the thereby determined effective ECS values comply with the ranges explicated by IPCC AR5, however now at the high-end.

20 **Keywords:** climate sensitivity, emulator, integrated assessment, mitigation scenarios, reduced climate models

## 1 Introduction

Climate-economy integrated assessment models (IAMs) represent an indispensable tool when deriving welfare-optimal climate policy scenarios (Kunreuther et al., 2014) or constrained welfare-optimal scenarios that would comply with a prescribed policy target (Clarke et al., 2014). Most of them employ relatively simple climate modules emulating highly 25 sophisticated climate models, Atmosphere-Ocean General Circulation Models (AOGCMs). These climate modules (called henceforth 'simple climate models' (SCMs)) offer computational efficiency and hence allow for projecting a broader set of scenarios in a reduced time. For IAMs based on a decision-analytic framework involving intertemporal welfare optimization, SCMs are indispensable as those IAMs' numerical solvers would call the climate module from ten thousands to hundred thousand times before numerical convergence is flagged.



The need to qualify the degree of accuracy of SCMs in mimicking AOGCMs or properly representing ensembles of AOGCMs is increasingly recognized (Calel & Stainforth, 2016; van Vuuren et al., 2011) as this might have immediate monetary consequences encoded in derived policy scenarios (Calel & Stainforth, 2016). Van Vuuren et al. (2011) found that IAMs tended to underestimate the effects of greenhouse gas emissions.

5 Due to centennial-scale quasi-linear properties of AOGCMs' global mean temperature (GMT) dynamics, SCMs have proven capable of emulating the behavior of AOGCMs regarding GMT change, deviations being a function of spread of forcing, SCM complexity and quality of SCM calibration. The climate component of MAGICC (Meinshausen et al., 2011) represents the most complex SCM currently in use. In some sense one could even call MAGICC an Earth System Model of Intermediate Complexity. Its ability to emulate all AOGCMs' GMT even more precisely than the standard deviation of  
10 interannual GMT variability has been demonstrated (Meinshausen et al., 2011), with a fixed set of parameters, utilized for the whole range of RCPs (representative concentration pathways, van Vuuren et al., 2011a). This represents the current gold standard of AOGCM emulation through SCMs.

Here we address the most extreme opposite end of scale of complexity within the model category of SCMs: the one-box model as introduced by Petschel-Held et al. (1999) (called 'PH99' from now on). Its role is as described in the following. By  
15 fitting PH99 to GMT time series one can utilize it as a diagnostic instrument as described in Andrews & Allen (2008). However its main application is functioning as an emulator of AOGCMs. In conjunction with the most parsimonious carbon cycle model (also described in Petschel-Held et al. (1999)) PH99 has been utilized for deriving 'admissible' greenhouse gas emission scenarios in view of prescribed GMT targets (Bruckner et al., 1999; Kriegler & Bruckner, 2004). Furthermore, the following climate-economic IAMs currently utilize PH99: FUND (Anthoff & Tol, 2014) and MIND (Edenhofer et al., 2005).  
20 While MIND has been succeeded by the IAM REMIND (Luderer et al., 2011) when it comes to spatial resolution or representing the energy sector by dozens of technologies, it currently serves as a state-of-the-art IAM for decision-making under uncertainty (Held et al., 2009; Lorenz et al., 2012; Neubersch et al., 2014; Roth et al., 2015) or joint mitigation-solar radiation management analyses (Roshan et al., 2016; Stankoweit et al., 2015).

Kriegler and Bruckner (2004) validated PH99 in conjunction with a simple carbon cycle model. When diagnosing the effect  
25 of the IS92a emissions scenario (Kattenberg et al., 1996) on GMT they demonstrated deviations of below 0.2 K for the 21<sup>st</sup> century (see their Fig.5).

None the less, we put forward that further validation is both necessary and possible on a higher level of consistency. Firstly, the respective GMT time series as checked in Kriegler and Bruckner (2004) is convexly increasing. However in the context of scenario generation compatible with the 2° target (UNFCCC, 2016) validation along GMT stabilization or even peaking  
30 scenarios is crucial, displaying a qualitatively different shape from IS92a. Secondly, in Kattenberg et al. (1996) the forcing was reconstructed by the auxiliary assumption of non-CO<sub>2</sub> greenhouse gas forcing approximately balancing aerosol cooling. Here we utilize recently diagnosed forcings for 14 CMIP('Coupled Model Intercomparison Project')5-AOGCMs by Forster et al. (2013). Finally we find current practice, directly prescribing equilibrium climate sensitivity (ECS) and a second, time-scale relevant property for calibrating PH99, inadequate in the context of 2° stabilization scenarios. Instead we propose to



calibrate PH99 in mapping those climate system properties on respective effective scenario-class-specific values before using them in PH99.

Hereby we comply with a quest recently formulated by Calel & Stainforth (2016): to establish application-specific re-calibration of PH99 as a valid future approach to emulation. Thereby PH99 could complement utilizing ever more complex climate modules, ranging from the two-box model of DICE (Nordhaus, 2013) to the rather complex upwelling-diffusion climate module of MAGICC (Meinshausen et al. (2013)). The benefit of PH99 would be two-fold: firstly, the most parsimonious SCM PH99 ensures maximum transparency. Secondly, in view of numerically solving decision-making under climate response uncertainty (Kunreuther et al., 2014), having to deal with dozens to thousands of alternative climate ‘states of the world’ in parallel poses a significant challenge for numerical solvers with regard to the available memory. In that regard PH99 appears particularly attractive.

The remainder of this article is organized as follows. Section 2 introduces our method of analysis, comprising of a 3-step procedure. (i) A traditional, if not naïve, calibration of PH99 by climate sensitivity and transient climate response (i.e. the GMT change in response to 1%/yr increase of the CO<sub>2</sub> concentration until doubling as against the pre-industrial value), (ii) a AOGCM-specific calibration, and (iii) the validation of the former. In Sect. 3 we first demonstrate that (i) would lead to emulation errors of up to 0.5 K for scenarios approximately compatible with the 2° target. We then show that this emulation error can generically be reduced to 0.1 K when choosing AOGCM-specific calibrations of PH99. This calibration is validated by an independent scenario. In Sect. 4 we show how PH99 can be calibrated for a given ECS, thereby avoiding AOGCM-specific calibrations. While this results in a larger emulation error than achieved in Sect. 3 (up to 0.2 K instead of up to 0.1 K), it would still suffice for most applications. In Sect. 5 we discuss the implications of our numerical findings for the integrated assessment community. In Sect. 6 we conclude and outline further research needs.

## 2 Method

The extensively used most parsimonious climate emulator is the one-box global energy balance model, Eq. (1), introduced by Petschel-Held et al. (1999), that projects the atmospheric GMT anomaly with respect to its preindustrial level. For a CO<sub>2</sub>-only forcing scenario, PH99 reads

$$25 \quad \dot{T} = \mu \ln(c) - \alpha T. \quad (1)$$

Hereby  $T$  denotes GMT,  $c$  is the CO<sub>2</sub> concentration in units of its pre-industrial level, and  $\alpha$  and  $\mu$  are constant tuning parameters.

From Eq. (1) we readily read ECS, the equilibrium temperature anomaly in response to a doubling of the CO<sub>2</sub> concentration as against its pre-industrial value:

$$30 \quad ECS = \frac{\mu}{\alpha} \ln(2) \quad (2)$$

also in line with Petschel-Held et al. (1999) and Kriegler and Bruckner (2004). In Appendix 1 we briefly derive TCR for this model:



$$TCR = \frac{\mu\gamma}{\alpha^2} \left( -1 + 2^{-\frac{\alpha}{\gamma}} + \frac{\alpha}{\gamma} \ln(2) \right). \quad (3)$$

Here,  $\gamma$  denotes a constant rate of increase of the  $\text{CO}_2$  concentration. In view of the current definition of TCR,  $\gamma$  amounts to 1%/yr.

In the following validation of PH99 is performed in three steps.

## 5 2.1 Step one: direct transfer of AOGCM characteristics

We first check whether simply calibrating PH99 from AOGCM-specific ECS and TCR data would deliver good emulations for  $2^\circ$ -target compatible scenarios. A technical difficulty arises from the fact that such scenarios are not available for  $\text{CO}_2$ -only forcing, but for various forcings. We address this difficulty by a chain of arguments along the equations as given below. As starting point we note that PH99 maps total radiative forcing onto temperature. We utilize scenarios generated from 14 AOGCMs (see Table 1) having participated in CMIP5, because the total forcings of these scenarios are reconstructed in Forster et al. (2013). ECS and TCR for those 14 models are taken from Forster et al. (2013), Table 1. Then model-specific  $\alpha$  and  $\mu$  are derived from Eq. (2) and Eq. (3).

In order to validate PH99, we need to drive Eq. (1) by the total forcing and compare the so derived emulator's GMT with the respective AOGCM's GMT. When inspecting Eq. (1) it becomes apparent that it still needs to be generalized from a  $\text{CO}_2$ -only to total forcing. We proceed accordingly in retrieving its physical interpretation. When multiplying it by a constant effective oceanic heat capacity  $h$ , we obtain an equation that governs the heat flux:

$$h \frac{dT}{dt} = -\alpha h T(t) + f(t) \quad (4)$$

Hence the  $\text{CO}_2$ -carrying summand ( $f(t)$ ) would become the  $\text{CO}_2$ -forcing and can now be generalized to the total forcing  $f$ . When dividing by the still to be determined factor  $h$ , we obtain:

$$20 \quad \frac{dT}{dt} = -\alpha T(t) + \frac{f(t)}{h} \quad (5)$$

In order to derive  $h$ , we re-consider the limiting  $\text{CO}_2$ -only case of Eq. (4):

$$h \frac{dT}{dt} = -\alpha h T(t) + Q_2 \frac{\ln c(t)}{\ln 2} \quad (6)$$

$Q_2$  denotes the additional forcing from the doubling of the  $\text{CO}_2$  concentration as against its pre-industrial value and is listed for all of the above AOGCMs (see Forster et al., 2013, Table 1). When comparing Eq. (1) and Eq. (6), we obtain:

$$25 \quad \mu = \frac{Q_2}{h \ln 2}. \quad (7)$$

Equation (7) is in-line with Kriegler & Bruckner (2004). Equation (7) allows for determining  $h$ , and in turn for time-integrating Eq. (5). Thereby from the AOGCMs' total climate forcing for the scenario RCP2.6, the temperature paths for the period 2006-2100 are projected.

To derive the initial levels (2006) of the temperature anomaly with respect to the preindustrial value, for each AOGCM we calculate the mean temperatures over the period 1881-1910 and 1991-2020, respectively, as the preindustrial level of



temperature and indicator for 2006 temperature level. The difference between these two is fixed as the initial temperature anomaly.

Each temperature trajectory should be compared to the temperature data from the related AOGCM. As for GMT-target-constrained economic optimizations (Clarke et al., 2014; Edenhofer et al., 2005) the maximum GMT (rather than the whole  
5 time series) is of special importance, as an error metric, the respective 2071-2100 GMT time averages of PH99 and AOGCM are subtracted. If the deviations are tolerable, the climate module is validated. We proceed with steps two and three if the deviations are found intolerable.

## 2.2 Step two: fitting PH99 to AOGCM scenarios

For each AOGCM,  $\alpha$  and  $\mu$  are tuned such that the deviations from the annual temperature data of RCP2.6 scenario for the  
10 period 2006-2100 are minimized in a least squares approach. For further diagnostics we then determine new ‘effective’ ECS and TCR from Eq. (2) and Eq. (3). As in step one, the deviations in 30-year means of GMT between PH99 and the respective APGCM are determined as an accuracy check.

In order to eliminate the effect of AOGCM drift, prior to a similar fitting exercise for MAGICC, Meinshausen et al. (2011) subtracted (low-pass filtered) control runs. We avoid accounting for AOGCM drift as our analysis is based on CMIP5  
15 AOGCMs (Forster et al., 2013) for which the problem of model drift has essentially been eliminated (Geoffroy et al., 2013, Fig.2). Furthermore, before comparing SCM and AOGCM time series, Meinshausen et al. (2011) low-pass filtered both with a cut-off frequency of 1/20 yrs. For the sake of parsimonious analysis we avoided low-pass filtering here as the one-box-only climate model PH99 essentially acts as a low-pass filter on the high frequency components of forcing. Therefore we decided to avoid introducing another degree of freedom in terms of a cut-off frequency into our analysis.

## 20 2.3 Step three: validation

Finally, we validate the PH99 model versions generated in step two. For this, independent temperature and forcing paths are needed to be run as a nontrivial test to check whether the trained climate module can accurately project other temperature data trajectories. To do so,  $\alpha$  and  $\mu$  determined in step two are implemented in PH99 the latter then being driven by the total climate forcing of the RCP4.5 scenario. Similar to steps one and two, the deviations in final 30-year means of GMT between  
25 PH99 and the respective APGCM are determined as an accuracy check.

## 3 Results

Table 1 shows the  $\alpha$  and  $\mu$  together with the feedback response time  $1/\alpha$  calculated in step one. For all of the indicators we also compute mean values and standard deviations of the samples. The mean value of ECS for GCM data is 3.35 K, with the minimum and maximum of 2.11 and 4.67, respectively. The mean value of timescales is 34.5 years.



Figure 1 represents the projected PH99 temperature evolution for the scenario RCP2.6 of each GCM in 2006-2100, using the data in Table 1 and forcings from RCP2.6. PH99 obviously overestimates the temperature anomaly for all GCMs during the last 30 years. The absolute values of the deviations of the mean temperature over the last 30 years, hereafter MTD, from AOGCM data are shown in Fig. 2. MTD ranges from 0.22 K for MRI-CGCM3 to about 0.79 K for HadGEM2-ES. On average, the deviations are about 0.45 K. This is clearly a large error, both in units of annual GMT standard deviation as well as the climate policy dimension. The signatories' of the Paris 2015 agreement (UNFCCC, 2016) stated goal is '...holding the increase in the global average temperature to well below 2°C above pre-industrial levels and pursuing efforts to limit the temperature increase to 1.5°C above pre-industrial levels...'. Hence a difference in 0.5 K does matter. Accordingly we proceed with step two.

10 In step two, we tune  $\alpha$  and  $\mu$  such that the deviations from the actual temperature of GCMs for the whole period 2006-2100 are minimized in a least square manner as represented in Fig. 3. From the thereby adjusted  $\alpha$  and  $\mu$  we derive ECS and TCR which are presented in Table 2. MTDs for the various AOGCMs are shown in Fig. 2.

From the results we find the following: Firstly, the average of absolute values of deviations is significantly reduced when  $\alpha$  and  $\mu$  are tuned. Indeed, the MTD average drops to below 0.02 K. Secondly, while the average of ECS decreases by 0.9 K from 3.35 K to 2.46 K, the average of TCR increases by 0.14 K from 1.90 K to 2.04 K. Thirdly, the mean value of feedback response times decreases significantly from about 35 years to below 12 years.

For validation we move on to step three. We utilize the RCP4.5 temperature and forcing data as provided by Forster et al. (2013). In Fig. 3 the respective GMT trajectories for any AOGCM are contrasted with the PH99-generated ones whereby  $\alpha$  and  $\mu$  are fixed to their value as determined in step two. MTDs are shown in Fig. 2. The results confirm that the climate module trained in the second step can appropriately mimic the temperatures estimated by the AOGCMs for RCP4.5, hence also out of the sample it was fitted to. As shown, the average value MTD is about 0.05 K. The deviations for three of the GCMs, namely CCSM4, CNRM-CM5, and NorESM1-M, are even better than the ones as diagnosed for RCP2.6 in step two.

#### 4 A mapping of $\alpha$ , $\mu$ , and ECS onto their PH99-specific counterparts

Finally, we attempt to abstract from fitting PH99 to individual AOGCMs and provide an approximate way to calibrate PH99 within the cloud of AOGCMs by simply knowing ECS. Then PH99 could be utilized for any ECS in analyses where ECS is uncertain. However, before diving into our suggestions, it is worthwhile that we first look at one of the existing options and utilize the curve suggested by Lorenz et al. (2012) which correlates  $\alpha$  and  $\mu$  to ECS. Using a sample from Frame et al. (2005) and assuming a strict relationship between  $1/\mu$  and ECS, Lorenz et al. (2012) suggest the following approximation:

$$\frac{1}{\mu} \approx \frac{1}{\bar{\mu}} - 10 \exp(-0.5 ECS) \quad (8)$$



where  $\bar{\mu}$  is the mean value of  $\mu$  in the sample (see Fig.7 in Lorenz et al., 2011, all quantities measured in the units utilized in Krieglner & Bruckner, 2004). Knowing  $\mu$ , Eq. (2) is used to determine  $\alpha$ . Equation (2) and Eq. (8) have been repeatedly used in the studies employing MIND and concerning uncertainties on ECS.

We employ Eq. (2) and Eq. (8) for all ECS from Table 1 and show the MTDs for the RCP2.6 scenario in Fig. 4. Obviously, on average, employing Lorenz's curve does not result in a better situation than step one. However hereby one might not have compared like with like. The two-dimensional uncertainty information as of Frame et al. (2005) was obtained by reconstructing the 20<sup>th</sup> century's warming signal from fingerprinting by means of a single AOGCM and then using these observational data as constraint. It is well-known that observational constraints may lead to different distributions than ensembles of AOGCMs would do (Andrews & Allen, 2008). Nevertheless we include this piece of information here to highlight that the two methods differ and a conscious decision is needed which one to use.

Given the inferred estimations shown in Table 2, one can directly relate  $\alpha$  and  $\mu$  to ECS. For this we generate polynomial fits (of orders 2 and 3) of  $\alpha$  and  $\mu$  against all AOGCM's ECSs. The attempt to predict a two-dimensional manifold from ECS alone implicitly exploits that AOGCM's TCRs can well be predicted from ECSs (see e.g. Meinshausen et al., 2009) in a statistical sense. Therefore, another option would be deriving  $\alpha$  and  $\mu$  analytically (as in the first step) when inferred ECS and TCR are correlated to ECS and TCR of AOGCMs.

Figure 5 relates  $\alpha$  and  $\mu$  (from Table 2) to ECS (from Table 1), using quadratic and cubic polynomial approximations. Figure 4 indicates that on average both approximations mimic the actual temperature paths better than a non-fitted one. The cubic estimation projects significantly smaller deviations compared to the quadratic approximation. The maximum MTD in the cubic approximation is about 0.3 K for IPSL-CM5A-LR, which is about a third of the maximum in the quadratic approximation that is revealed for CSIRO-Mk3-6-0.

In the following we describe alternative ways to extrapolate from the 14 utilized AOGCMs on any ECS, going beyond the scheme displayed in Fig. 4. As one option, shown in Fig. 6, we linearly regress ECS and TCR values inferred from step two against their original AOGCM counterparts respectively and obtain

$$ECS_{PH99} \approx a ECS_{AOGCM} + b \quad (9)$$

with  $a=0.5846$ ,  $b=0.5095$  K, and R-square=0.8158, as long as  $ECS_{PH99} < ECS_{AOGCM}$

and

$$TCR_{PH99} \approx c TCR_{AOGCM} + d \quad (10)$$

with  $c=0.9763$ ,  $d=0.1829$  K, and R-square=0.667.

Another option is using Eq. (9) along with a linearly regressed  $TCR_{PH99}$  over  $ECS_{AOGCM}$ , that is

$$TCR_{PH99} \approx m ECS_{AOGCM} + n \quad (11)$$

with  $m=0.4582$ ,  $n=0.5044$  K, and R-square=0.7876.

The respective MTDs are shown in Fig. 4. Although both approximations mimic the actual temperature paths better than a non-fitted one, regressing both inferred effective ECS and TCR solely against AOGCMs' ECS (hereafter, ETE, shown in Blue in Figure 4) obviously is the overall better approximation.



The use of ETE has a three-fold advantage over all other options described above, especially for the IAM community. Firstly, its approximation is better than all options but the cubic fit. Even though the cubic fit may give a better approximation in our analysis it is only better by 0.03 K. Still the ETE has an advantage over it because, secondly, one can easily make use of broader range of climate sensitivities, for example, ranging from 1 K to 9 K, which may not be accurately  
5 determined by the cubic fit. Lastly, by use of ETE, not only it projects a better approximation, but also prior probabilistic knowledge on TCR is not a necessary input – which is convenient if not yet available.

## 5 Discussion

Why are GMT scenarios generated from PH99 biased towards higher temperatures? In the literature it has been discussed, for decades, that in systems more complex than just one box, transient warming dynamics are governed by a ‘transient  
10 climate sensitivity’ markedly lower than ECS (for an overview see, e.g. Meinshausen et al., 2011, in conjunction with their Fig.1). Andrews & Allen (2008) warned against straightforward usage of PH99 in that regard. However these diagnostics mainly referred to convexly increasing GMT paths while RCP2.6 leads to quasi-stabilizing GMT paths.

Hence additional mechanisms for explanation should not be ruled out ex ante. This means, that, firstly, the statistical errors in determining AOGCMs’ ECS, TCR, and  $Q_2$  may lead, mediated through the nonlinear mapping on PH99’s parameters, to  
15 an overall bias in PH99’s GMT. Furthermore, diagnosing the total radiative active in an AOGCM is a complex issue (see e.g. again Meinshausen et al., 2011, for a discussion). A bias to the high-end here would also result in too large GMT responses by PH99.

However, assuming that all AOGCM-based inputs into the current analysis were unbiased, our findings would imply that past integrated assessment studies based on PH99 implicitly worked with ECS values that were larger than announced, as  
20 shown in Fig. 6. Since Lorenz et al. (2012), the probability density function by Wigley & Raper (2001), a log-normal function, has been utilized within the MIND model. In the remainder of this paragraph we argue why we would also prefer log-normal distributions for ECS in the future. The rationale behind using a log-normal function is our personal conviction that constraining ECS by paleo data in addition to instrumental records results in thin-tailed distributions. This conviction rests on an approach successfully applied at an Earth system model of intermediate complexity (Schneider von Deimling et  
25 al., 2006). In contrast, relying solely on the instrumental record must result in fat-tailed distributions (Roe & Baker, 2007). However constraining ECS by paleo data still does not seem to be on the same level of quality than doing so by the modern instrumental record. A log-normal distribution would then describe the borderline case of a fat and a thin tail, hence expresses mainly relying on the observational record, but also allowing for Bayesian learning from paleo data.

Suppose we accepted above suggestion to map ECS values onto effective, scenario class-adjusted values before usage in  
30 PH99. Would a re-scaled version of that lognormal distribution still comply with our recent knowledge on ECS? The 5%, 50%, and 95%-quantiles of the log-normal distribution by Wigley & Raper (2001) are 1.2 K, 2.6 K, and 5.8 K, respectively. When interpreting these values as PH99 values, as they have been in fact utilized in PH99 since Lorenz et al. (2012) for the





MIND model, one could ask for the back-transformed ECS values according to our Fig. 6. The respective values are 1.2 K, 3.6 K, and 9.0 K. From Fig. 7, from the IPCC AR5's synopsis of current knowledge on ECS (Bindoff et al., 2013) we see that these are still in-line with the range spanned by instrumental studies. Hence the results obtained by PH99 in conjunction with the distribution by Wigley & Raper (2001) are not erroneous, but simply need to be re-interpreted as rather high-end representatives within the collection of ranges as described in IPCC AR5.

In fact Fig. 6 might even exaggerate the need for correcting ECS and TCR values. As we purposely avoided usage of a low-pass filter before fitting PH99 to AOGCMs output, improved goodness of fit was obtained for slightly emulating natural variability (see the small wiggles of PH99-scenarios as displayed in Fig. 3). This in turn might have led to too small inferred feedback response times which usually correlate with too low ECS values. Future work will include a sensitivity study regarding the effects of cut-off frequency of low-pass filtering. However this possibility cannot eliminate the apparent need to re-interpret ECS and TCR of PH99, as it is obvious from our observed emulator-AOGCM difference of 0.5 K in GMT (see Fig. 1).

Furthermore, if such a transformation were found necessary by future work, how would one generate it? Our paper solely rests on the properties of 14 CMIP5 AOGCMs that may not sample our current joint distribution of ECS/TCR well. In fact Andrews & Allen (2008) pointed to the possibility that ensembles of GCMs misrepresented an actual joint distribution as inferred from the instrumental record. Hence we propose deriving two separate transformation schemes: one for a specified set of AOGCMs as our current work does and a further one for probabilistic information generated from relating a state-of-the-art SCM or Earth system model of intermediate complexity to the instrumental record (examples for the latter: see the probabilistic studies as cited in Fig. 7).

In any case such transformation rules must be able to tackle the whole range of potential ECS and TCR values in order to enable us to transform density functions. Quite the contrary, our rather pragmatic polynomial fit as of Fig. 5 should not be extrapolated beyond the range spanned by the 14 AOGCMs utilized in this study. Particularly a 3<sup>rd</sup> order polynomial would generate unphysical effects. Furthermore such a transformation should treat ECS and TCR as independent entities, while we treated ECS as the only predictor in Fig. 4 and Fig. 5, just to demonstrate the chance of finding a model-independent transformation.

Finally when adjusting PH99 according to such a transformation or even directly fitting to time series of an AOGCM, PH99 can emulate an AOGCM to a sufficient level of accuracy. Hereby we utilized RCP2.6 scenarios for fitting, and RCP4.5 scenarios for validation. As economic optimizers would, in any practical sense, employ only variations of RCP2.6 scenarios when finding a constrained welfare optimum compatible with the 2° target, those deviations from the RCP2.6 scenario would generically be an order of magnitude smaller than the difference as against the RCP4.5 scenario used for validation. If emulation quality for the RCP4.5 scenario were sufficient, the more so we expect sufficiency for scenarios approximately in-line with the 2° target!



## 6 Summary and Conclusion

We utilize recent data on total radiative forcing (Forster et al., 2013) of 14 CMIP5 state-of-the-art Atmosphere Ocean General Circulation Models (AOGCMs) in order to test the validity of the one-box climate module by Petschel-Held (1999, ‘PH99’) for scenarios approximately compatible with the 2° target. PH99 is currently utilized within the integrated assessment models FUND and MIND.

We find that when prescribing equilibrium climate sensitivity (ECS) and transient climate response (TCR) of these AOGCMs to the emulator PH99, generally leads to an overestimation of global mean temperature (GMT) by 0.5 K. Quite the contrary, when directly fitting PH99 to RCP2.6 time-series and validating by RCP4.5 series, we find that PH99 can emulate AOGCMs to a degree of accuracy better than 0.1 K.

We propose several explanations for the intolerable discrepancy of emulators and AOGCM when directly prescribing ECS and TCR. The first candidate to be checked in future investigations would be RCP2.6 scenarios being characterized by transient climate sensitivities markedly smaller than ECS, as already known for purely convex temperature scenarios.

However we find that PH99 can be used for emulating AOGCMs within an accuracy of 0.1 K to 0.2 K if its ECS and TCR are re-interpreted as effective, 2°C-scenario-class specific values and mapped from original ECS and TCR values. We suggest a first version of such a mapping.

Older work based on PH99, executed within FUND and MIND may need to be re-interpreted in the sense that higher values of ECS had effectively been operated. For the MIND model, even re-interpreted values of ECS are still within the range outlined by IPCC AR5 (see Fig. 7).

For future work, we propose the following steps: (i) It has to be checked to what extent the transformations on ECS and TCR we found are robust under low-pass filtering scenarios before fitting. (ii) By comparison with more sophisticated, multi-box climate modules it should be tested whether the effect of a transient climate sensitivity (and TCR) alone could explain our observed PH99-AOGCM discrepancy. (iii) Future discussions with the AOGCM community should illuminate to what extent the further explanations we suggested might also apply, potentially reducing the correction need for PH99. (iv) An AOGCM-independent, yet scenario-class-specific 2-dimensional mapping from ECS/TCR onto ECS/TCR designed for PH99, should be derived in conjunction with two-dimensional distributions inferred from observations as done in Frame et al. (2005). The IAM community could then be offered both options for emulation, the one presented here, trained by AOGCMs, and the one based on observational data and mediated via more complex SCMs.

Thus in both cases, the use of PH99 could be continued as the most parsimonious emulator of AOGCMs, especially efficient for decision-making under climate response uncertainty.

## 30 Appendix: An Analytic Expression for TCR within PH99

We recapitulate Eq. (1) as

$$\dot{T} = \mu \ln(c) - \alpha T \tag{A1}$$



TCR is defined as the temperature change in response to a 1%/yr increase in CO<sub>2</sub> concentration, starting from preindustrial conditions. Hence the concentration, expressed in units of the pre-industrial concentration, reads

$$c = \exp(\gamma t) \quad (\text{A2})$$

5 hereby  $\gamma$  denoting the above rate of change. As Eq. (A1) represents a linear ordinary differential equation with constant coefficients, and the initial temperature anomaly vanishes, its solution reads

$$T = \mu\gamma \exp(-\alpha t) \int t \exp(\alpha t) dt = \frac{\exp(-\alpha t) \mu\gamma(1 + \exp(\alpha t).(-1 + \alpha t))}{\alpha^2} \quad (\text{A3})$$

Temperature should be evaluated at  $t_2$  when the concentration is doubled.  $t_2$  is determined by  $c(t_2)=2 \Rightarrow t_2=\ln 2/\gamma$ . From this and Eq. (A3) we conclude Eq. (3). (In fact we retrieve the same result from an expression given in Andrews & Allen, 2008, when we plug in our expression for  $t_2$  into their expression that is phrased in terms of ECS.)

## 10 Authors' Contributions

M.M.K. did the analysis, wrote the codes, and prepared the visualizations. H.H. suggested and developed step one of the analysis, M.M.K. suggested and developed the alternative scheme. H.H. wrote the framing sections of the manuscript, M.M.K. wrote the descriptive and analysing sections.

## Competing Interests

15 The authors declare that they have no conflict of interest.

## Acknowledgments

The authors would like to thank J. Marotzke for pointing them to the Forster et al. (2013) article, discussing these results on total forcing and providing the relevant data. In addition, the authors would like to thank C. Li for supporting the data handling process and pointing the authors to Geoffroy et al. 2013 describing negligible AOGCM drift. The authors are also  
20 grateful to E. Roshan for her help on visualization and providing quantiles of Wigley's & Raper's (2001) distribution on ECS and to B. Blanz for carefully reading the manuscript. M.M.K. has been supported by the Cluster of Excellence 'Integrated Climate System Analysis and Prediction' (CliSAP, DFG-EXC177).

## References

Andrews, D. G. and Allen, M. R.: Diagnosis of climate models in terms of transient climate response and feedback response  
25 time, Atmospheric Science Letters, 9, 7–12, 2008.



- Anthoff, D. and Tol, R. S. J.: The Climate Framework for Uncertainty, Negotiation and Distribution (FUND): Technical description, Version 3.6, retrieved November, 2013.
- Bindoff, N. L., Stott, P. A., AchutaRao, K. M., Allen, M. R., Gillett, N., Gutzler, D., Hansingo, K., Hegerl, G., Hu, Y., Jain, S., and others: Detection and attribution of climate change: From global to regional, 2013.
- 5 Bruckner, T., Petschel-Held, G., Leimbach, M., and Toth, F. L.: Methodological aspects of the tolerable windows approach, *Climatic Change*, 56, 73–89, 2003.
- Bruckner, T., Petschel-Held, G., Leimbach, M., and Toth, F. L.: Methodological aspects of the tolerable windows approach, *Climatic Change*, 56, 73–89, 2003.
- Calel, R. and Stainforth, D. A.: On the Physics of three Integrated Assessment Models, *Bull. Amer. Meteor. Soc.*,  
10 doi:10.1175/BAMS-D-16-0034.1, 2016.
- Clarke, L., Jiang, K., Akimoto, K., Babiker, M., Blanford, G., Fisher-Vanden, K., Hourcade, J.-C., Krey, V., Kriegler, E., Löschel, A., and others: Assessing transformation pathways, 2014.
- Geoffroy, O., Saint-Martin, D., Olivié, D. J. L., Voldoire, A., Bellon, G., and Tytéca, S.: Transient Climate Response in a Two-Layer Energy-Balance Model. Part I: Analytical Solution and Parameter Calibration Using CMIP5 AOGCM  
15 Experiments, *J. Climate*, 26, 1841–1857, doi:10.1175/JCLI-D-12-00195.1, 2013.
- Kattenberg, A., Giorgi, F., Grassl, H., Meehl, G. A., Mitchell, J. F., Stouffer, R. J., Tokioka, T., Weaver, A. J., and Wigley, T. M.: Climate models—projections of future climate, *Climate Change 1995: The Science of Climate Change. Contribution of Working Group I to the Second Assessment Report of the Intergovernmental Panel on Climate Change*, 285–357, 1996.
- Kriegler, E. and Bruckner, T.: Sensitivity analysis of emissions corridors for the 21st century, *Climatic Change*, 66, 345–  
20 387, 2004.
- Kunreuther, H., Gupta, S., Bosetti, V., Cooke, R., Dutt, V., Ha-Duong, M., Held, H., Llanes-Regueiro, J., Patt, A., Shittu, E., and others: Integrated risk and uncertainty assessment of climate change response policies, 2014.
- Lorenz, A., Schmidt, M. G. W., Kriegler, E., and Held, H.: Anticipating Climate Threshold Damages, *Environ Model Assess*, 17, 163–175, doi:10.1007/s10666-011-9282-2, 2012.
- 25 Luderer, G., Leimbach, M., Bauer, N., and Kriegler, E.: Description of the ReMIND-R model, Potsdam Institute for Climate Impact Research. Retrieved from: [https://www.pik-potsdam.de/research/sustainable-solutions/models/remind/REMIND\\_Description.pdf](https://www.pik-potsdam.de/research/sustainable-solutions/models/remind/REMIND_Description.pdf), 2011.
- Meinshausen, M., Raper, S. C. B., and Wigley, T. M. L.: Emulating coupled atmosphere-ocean and carbon cycle models with a simpler model, *MAGICC6 – Part 1: Model description and calibration*, *Atmos. Chem. Phys.*, 11, 1417–1456,  
30 doi:10.5194/acp-11-1417-2011, 2011.
- Meinshausen, M., Meinshausen, N., Hare, W., Raper, S. C. B., Frieler, K., Knutti, R., Frame, D. J., and Allen, M. R.: Greenhouse-gas emission targets for limiting global warming to 2 C, *Nature*, 458, 1158–1162, 2009.
- Nordhaus, W. D.: *The climate casino: Risk, uncertainty, and economics for a warming world*, Yale University Press, 2013.



- Petschel-Held, G., Schellnhuber, H.-J., Bruckner, T., Toth, F. L., and Hasselmann, K.: The tolerable windows approach: Theoretical and methodological foundations, *Climatic Change*, 41, 303–331, 1999.
- Roe, G. H. and Baker, M. B.: Why is climate sensitivity so unpredictable?, *Science (New York, N.Y.)*, 318, 629–632, 2007.
- Roshan, E., Mohammadi Khabbazan, M., Held, H.: A Scheme For Jointly Trading Off Costs And Risks Of Solar Radiation Management And Mitigation Under Long-Tailed Climate Sensitivity Probability Density Distributions, EAERE Zurich, 22-25 June 2016.
- Roth, R., Neubersch, D., Held, H.: Evaluating Delayed Climate Policy by Cost-Risk Analysis, EAERE Helsinki, 24-27 June 2015.
- Schneider von Deimling, T., Held, H., Ganopolski, A., and Rahmstorf, S.: Climate sensitivity estimated from ensemble simulations of glacial climate, *Clim Dyn*, 27, 149–163, doi:10.1007/s00382-006-0126-8, 2006.
- Stankoweit, M., Schmidt, H., Roshan, E., Pieper, P., and Held, H.: Integrated mitigation and solar radiation management scenarios under combined climate guardrails, in: EGU General Assembly Conference Abstracts, 7152, 2015.
- van Vuuren, D. P., Edmonds, J. A., Kainuma, M., Riahi, K., and Weyant, J.: A special issue on the RCPs, *Climatic Change*, 109, 1–4, doi:10.1007/s10584-011-0157-y, 2011.
- van Vuuren, D. P., Lowe, J., Stehfest, E., Gohar, L., Hof, A. F., Hope, C., Warren, R., Meinshausen, M., and Plattner, G.-K.: How well do integrated assessment models simulate climate change?, *Climatic Change*, 104, 255–285, doi:10.1007/s10584-009-9764-2, 2011.
- Wigley, T. M. and Raper, S. C.: Interpretation of high projections for global-mean warming, *Science (New York, N.Y.)*, 293, 451–454, doi:10.1126/science.1061604, 2001.



**Table 1: PH99 parameters ( $\alpha$  and  $\mu$ ) and feedback response times ( $1/\alpha$ ) utilizing data ( $ECS$  and  $TCR$ ) from AOGCMs.**

	PH99 Parameters		Climate Sensitivities		Feedback Response Times
	$\alpha$ [1/yr]	$\mu$ [K/yr]	$ECS$ [K]	$TCR$ [K]	$1/\alpha$ [yr]
bcc_csm1_1_m	0.052	0.217	2.87	2.10	19.1
bcc_csm1_1	0.033	0.132	2.82	1.70	30.8
CanESM2	0.038	0.204	3.69	2.40	26.1
CCSM4	0.035	0.145	2.89	1.80	28.7
CNRM_CM5	0.038	0.177	3.25	2.10	26.5
CSIRO_Mk3_6_0	0.019	0.111	4.08	1.80	53.2
GISS_E2_R	0.048	0.147	2.11	1.50	20.8
HadGEM2_ES	0.027	0.177	4.59	2.50	37.4
IPSL_CM5A_LR	0.022	0.130	4.13	2.00	45.9
MIROC5	0.027	0.107	2.72	1.50	36.6
MIROC_ESM	0.021	0.140	4.67	2.20	48.0
MPI_ESM_LR	0.027	0.143	3.63	2.00	36.7
MRI_CGCM3	0.034	0.127	2.60	1.60	29.5
NorESM1_M	0.023	0.093	2.80	1.40	43.5
<b>Multimodel Mean</b>	<b>0.032</b>	<b>0.146</b>	<b>3.35</b>	<b>1.90</b>	<b>34.5</b>
<b>Standard Deviation</b>	<b>0.010</b>	<b>0.036</b>	<b>0.792</b>	<b>0.342</b>	<b>10.350</b>



**Table 2: PH99 parameters ( $\alpha$  and  $\mu$ ), climate sensitivities ( $ECS$  and  $TCR$ ), and feedback response times ( $1/\alpha$ ) after fitting PH99 GMT time series to AOGCM RCP2.6 GMT time series.**

	PH99 Parameters		Climate Sensitivities		Feedback Response Times
	$\alpha$ [1/yrs]	$\mu$ [K/yrs]	$ECS$ [K]	$TCR$ [K]	$1/\alpha$ [yrs]
bcc_csm1_1_m	0.058	0.199	2.37	1.79	17.20
bcc_csm1_1	0.080	0.267	2.32	1.90	12.51
CanESM2	0.093	0.377	2.81	2.37	10.74
CCSM4	0.082	0.264	2.24	1.85	12.21
CNRM_CM5	0.084	0.329	2.73	2.26	11.97
CSIRO_Mk3_6_0	0.079	0.280	2.45	2.00	12.61
GISS_E2_R	0.345	0.746	1.50	1.44	2.90
HadGEM2_ES	0.114	0.485	2.94	2.57	8.75
IPSL_CM5A_LR	0.046	0.201	3.01	2.11	21.58
MIROC5	0.158	0.455	1.99	1.81	6.32
MIROC_ESM	0.096	0.478	3.45	2.93	10.41
MPI_ESM_LR	0.088	0.344	2.70	2.26	11.33
MRI_CGCM3	0.059	0.178	2.09	1.58	16.93
NorESM1_M	0.105	0.292	1.92	1.66	9.49
<b>Multimodel Mean</b>	<b>0.106</b>	<b>0.350</b>	<b>2.46</b>	<b>2.04</b>	<b>11.78</b>
<b>Standard Deviation</b>	0.074	0.152	0.512	0.409	4.639

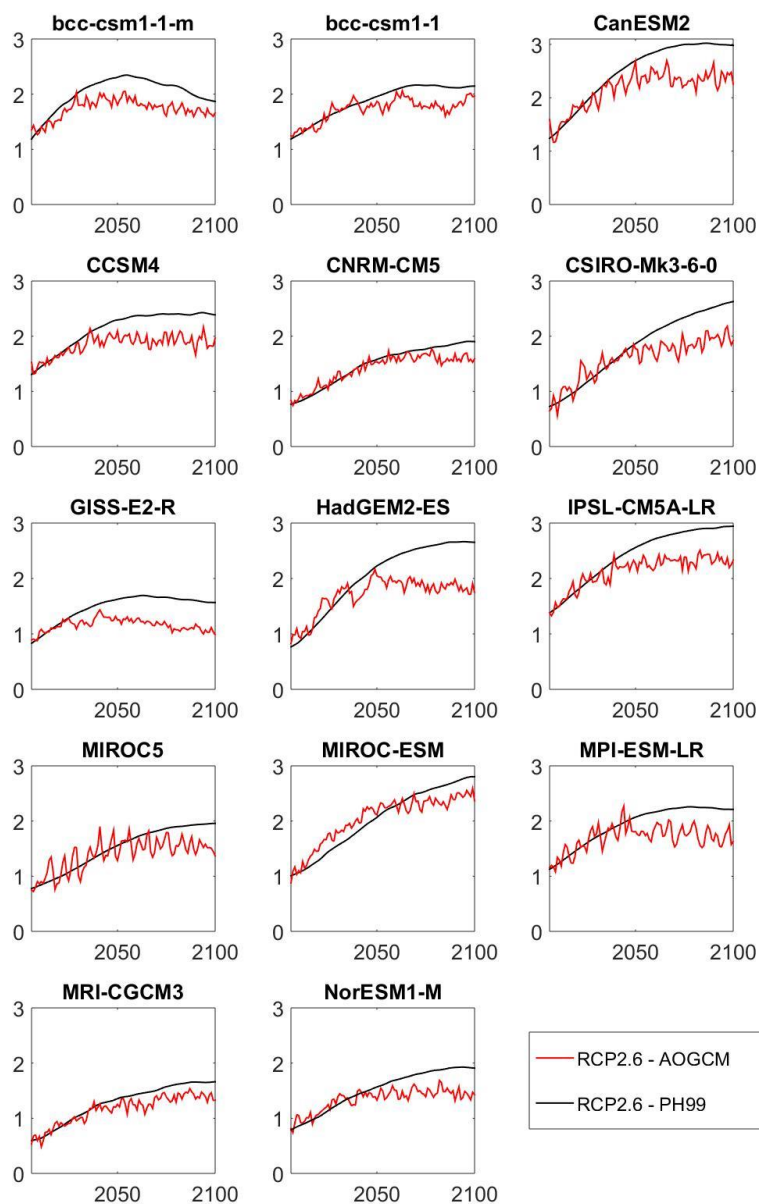


**Figure 1:** The comparison of temperature paths projected by PH99 (black curve), calibrated by AOGCM's ECS and TCR, to the corresponding AOGCM's temperature paths (red curves). Deviations on the order of 0.5 K for 2100 are observed.



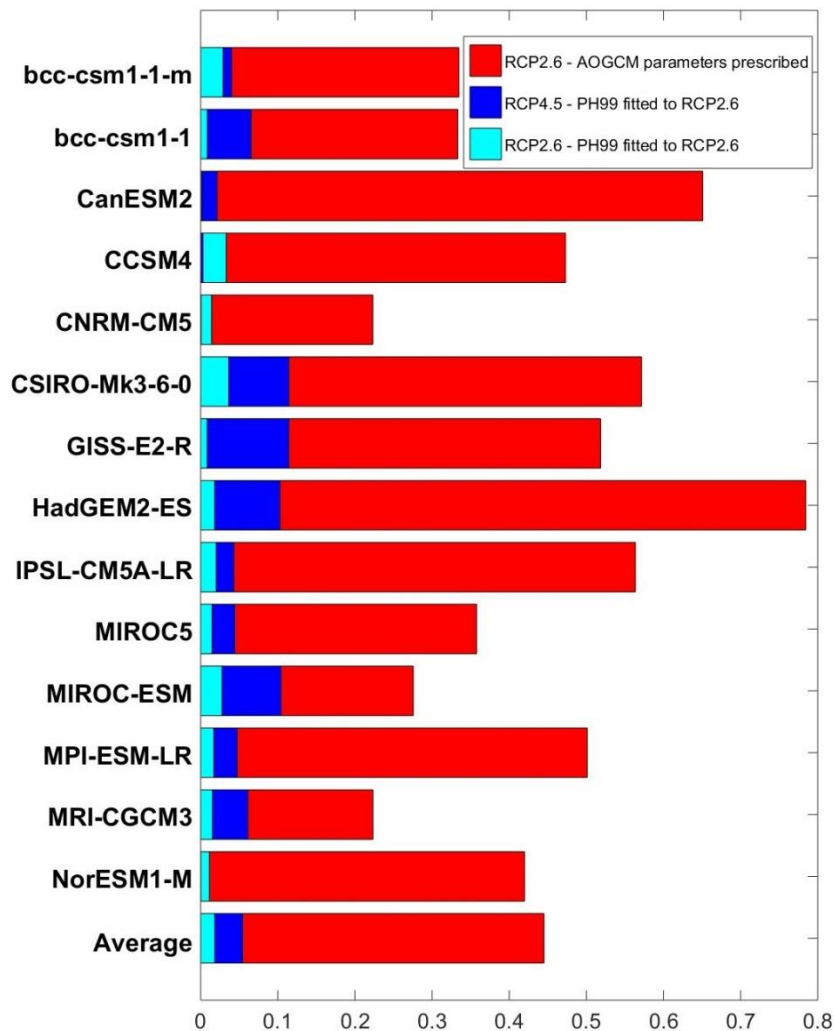
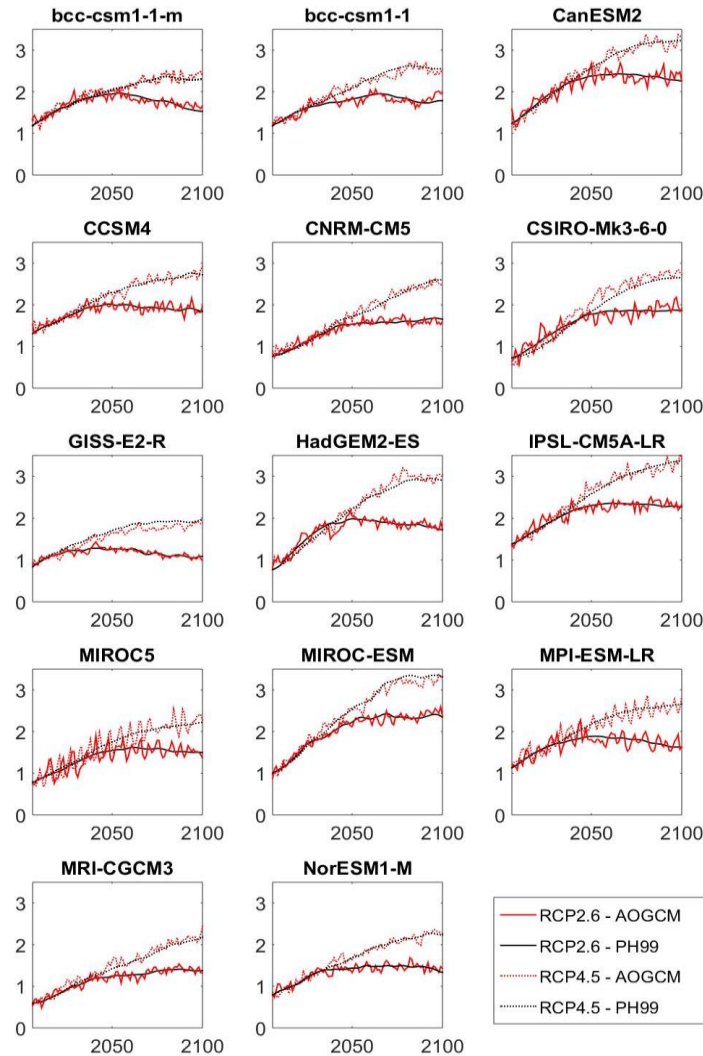


**Figure 2: Modulus of deviations of PH99 last 30 years GMT mean values from corresponding AOGCM means. The red bars show the deviations for RCP2.6 when  $\alpha$  and  $\mu$  are from Table 1 and not fitted. The cyan bars show the deviations in RCP2.6 when  $\alpha$  and  $\mu$  are fitted to AOGCMs RCP2.6 data. The blue bars show the deviations for RCP4.5 when  $\alpha$  and  $\mu$  are kept as before (validation).**



5 **Figure 3: The comparison of temperature evolutions projected by the climate module PH99 (black solid and dotted curves) to the actual AOGCM's temperature (red solid and dotted curves).  $\alpha$  and  $\mu$  are tuned to fit the PH99 temperature path (black solid curve) to the respective AOGCM RCP2.6 temperature paths (red solid curve). Using the fitted  $\alpha$  and  $\mu$ , and taking the forcing reconstructed for RCP4.5, PH99 also reproduces the projected RCP4.5 (black dotted curves). Red dotted curves show the actual RCP4.5 temperatures. Hence the validation is successful.**

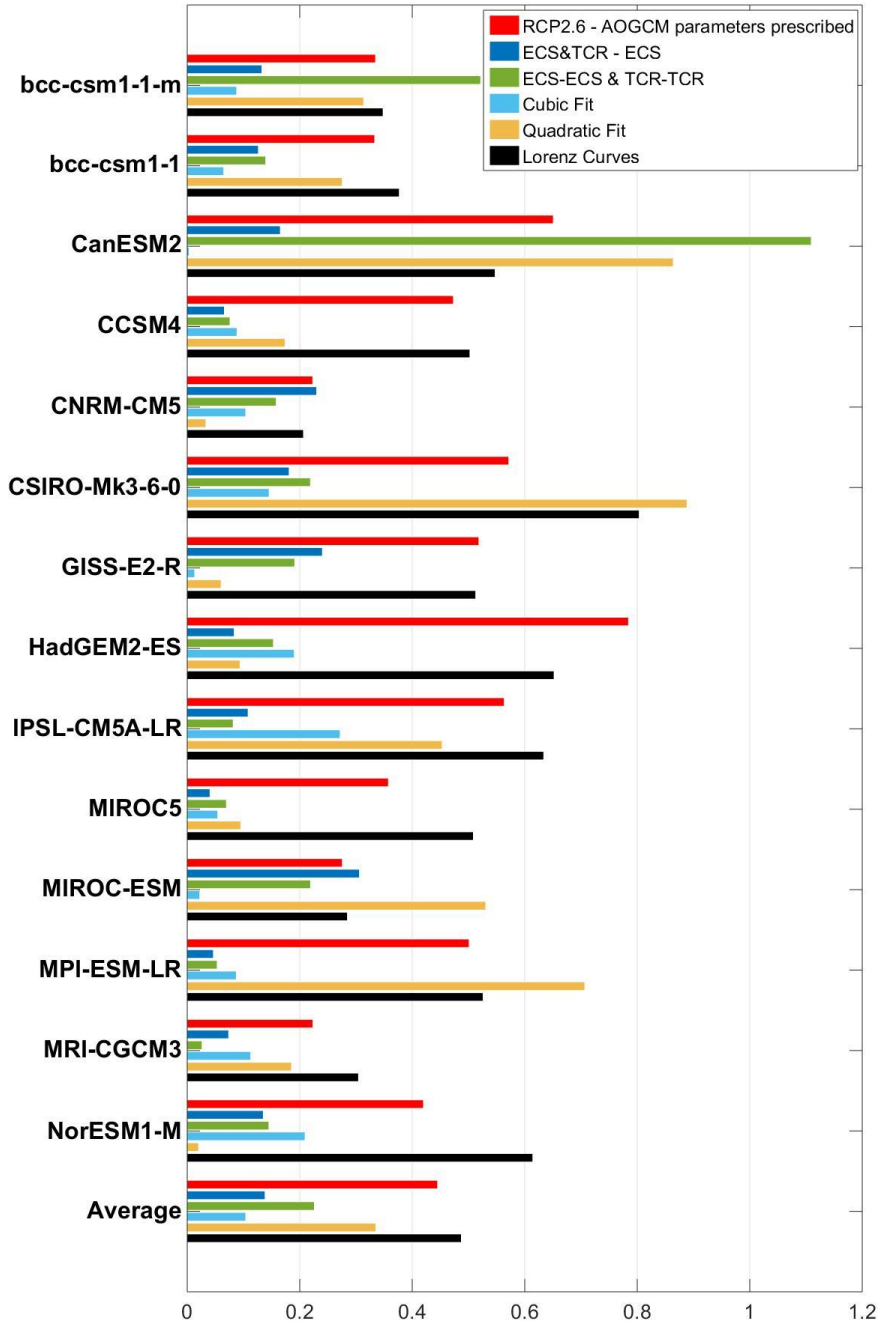


Figure 4: Modulus of mean temperature deviations over the last 30 years (MTD) PH99 vs. AOGCMs when  $\alpha$ ,  $\mu$ , ECS, and TCR from Table 2 are related to ECS and TCR in Table 1. Using quadratic (orange bars) and cubic functions (cyan bars),  $\alpha$  and  $\mu$  are related to ECS. Using linear fits, ECS and TCR are related to ECS (blue bars). Using linear fits, ECS and TCR are related to ECS and TCR respectively (green bars). The red bars show the deviations for RCP2.6 when  $\alpha$  and  $\mu$  are from Table 1 and not fitted (the same as Fig.2). The black bars indicate MTD using Lorenz's curve.

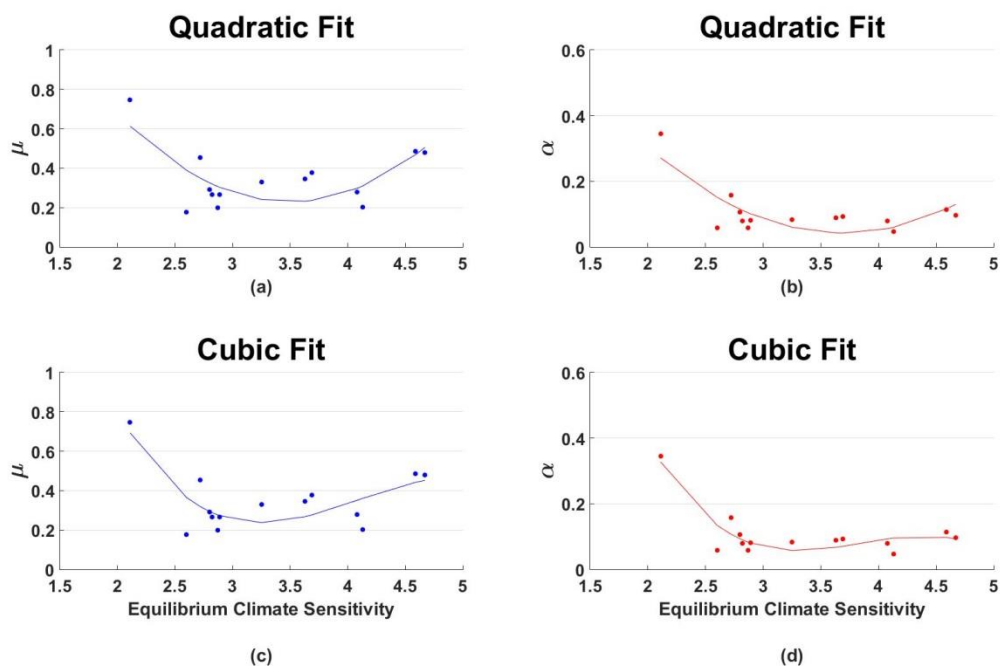
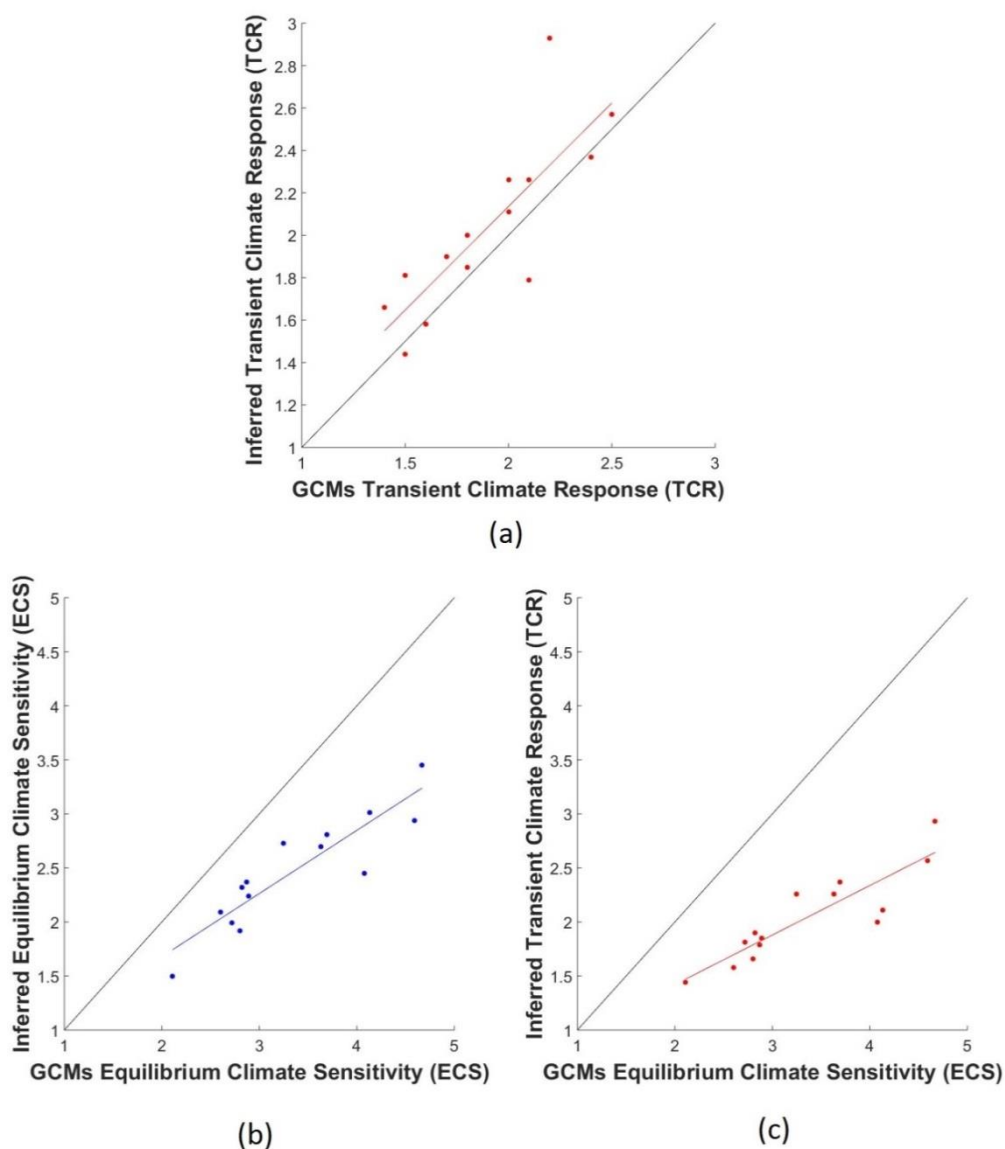


Figure 5: Quadratic (up) and cubic (down) relationships of  $\mu$  (left) and  $\alpha$  (right) in Table 2 to ECS in Table 1.



**Figure 6:** Inferred effective TCR vs. AOGCMs' TCR (a), inferred effective ECS vs. AOGCMs' ECS (b), and inferred effective TCR vs. AOGCMs' ECS (c). While TCRs differ by less than 0.2 K, ECSs differ by up to 2 K. This opens the door for a discussion whether PH99 should be calibrated by scenario class-adjusted effectively lower values of ECS.

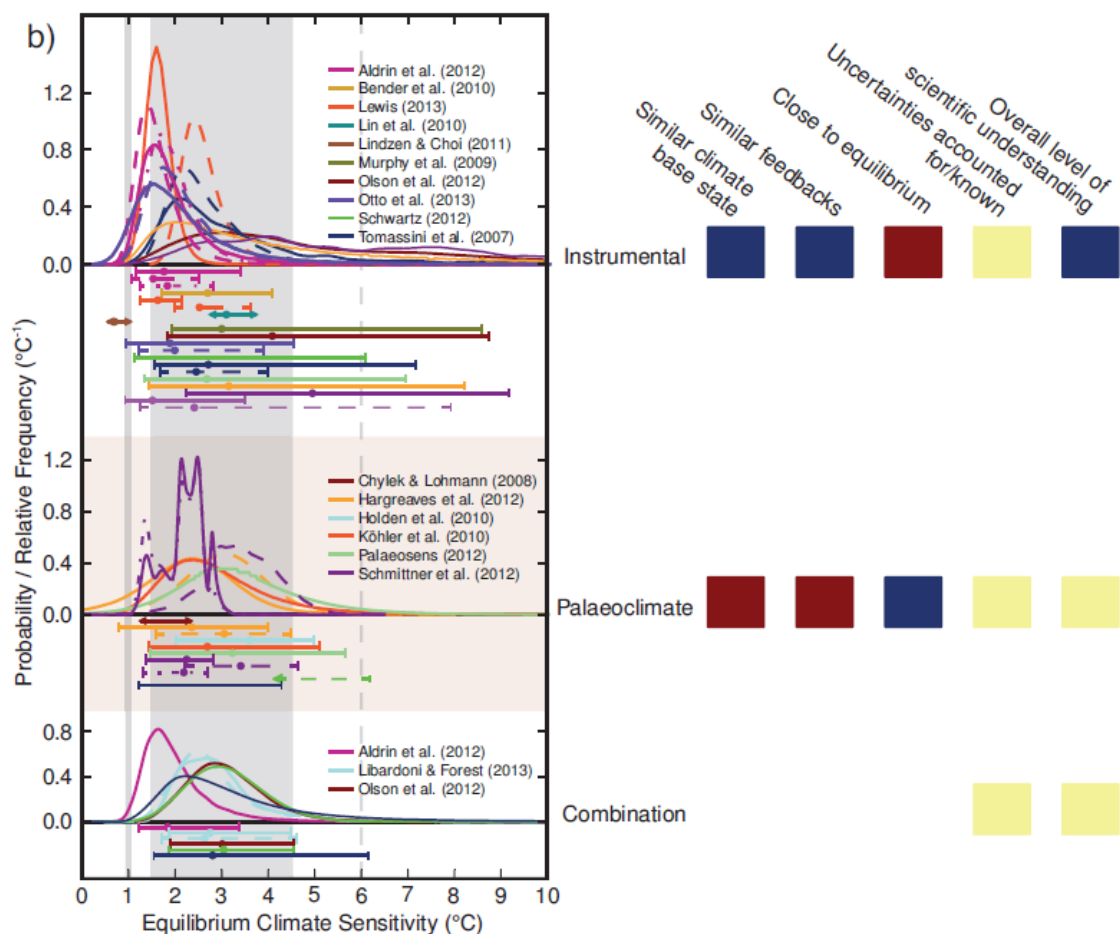


Figure 7: Probability density distributions of ECS according to IPCC AR5 WG-I (Bindoff et al., 2013, Fig. 10.20).